Biomechan Model Mechanobiol (2006) 5: 227–236
DOI 10.1007/s10237-005-0010-1

ORIGINAL PAPER

J.-F. Bolduc · L.J. Lewis
C.-É. Aubin · A. Geitmann

Finite-element analysis of geometrical factors in micro-indentation of pollen tubes

Received: 8 June 2005 / Accepted: 6 November 2005 / Published online: 3 March 2006

Abstract Micro-indentation is a new experimental approach to assess physical cellular properties. Here we attempt to quantify the contribution of geometrical parameters to a cylindrical plant cell's resistance to lateral deformation. This information is important to correctly interpret data obtained from experiments using the device, such as the local cellular stiffness in pollen tubes. We built a simple finite-element model of the micro-indentation interacting partners – micro-indenter, cell (pollen tube), and underlying substratum, that allowed us to manipulate geometric variables, such as geometry of the cell, cell radius, thickness of the cell wall and radius of the indenting stylus. Performing indentation experiments on this theoretical model demonstrates that all four parameters influence stiffness measurement and can therefore not be neglected in the interpretation of micro-indentation data.

1 Introduction

An integrative approach to understanding the biology of the cell cannot be confined to biochemical and genetic processes; it has to take into account the mechanical interaction between cellular components. The importance of the mechanical aspects of cell biology is evident in cellular functions such as mechanotransduction, in which biochemical signaling cascades are triggered upon mechanical stimulation of a cell. Cellular architecture is determined essentially by the interaction between the cytoskeletal elements and the plasma membrane. The architecture of plant cells is more complex due to the presence of two additional structural features: the cell wall – a more or less stiff extracellular matrix surrounding the cell – and the turgor – a hydrostatic pressure whose establishment depends on the presence of the cell wall.

To understand the physical properties and the mechanical interactions between these structural components, various techniques have been used in the past. All of them had the purpose to measure physical properties of individual cellular components or structural entities on subcellular level. They include magnetic twisting cytometry (Bao and Suresh 2003; Fabry et al. 2001), ball tonometry (Lintilhac et al. 2000; Wei et al. 2001), micro-manipulation (Thomas et al. 2000; Wang et al. 2004), micropipette aspiration (Jones et al. 1999), atomic force microscopy (AFM) (Hassan et al. 1998), optical tweezers (Bao and Suresh 2003), cytoindentation (Shin and Athanasiou 1999), and turgor pressure probe (Tomos 2000). Another powerful tool that has delivered very interesting data is micro-indentation. The principle of this technique is similar to that used in AFM as it is based on a cantilever, the deformation of which gauges the local cellular stiffness. The difference lies in the experimental setup and the scale of deformations which is an order of magnitude above that common for AFM. Micro-indentation has been applied to both animal cells (Petersen et al. 1982; Zahalak et al. 1990) and plant cells (Geitmann and Parre 2004; Geitmann et al. 2004; Parre and Geitmann 2005a,b). In animal cells, local deformations carried out by micro-indentation essentially measure the resistance exerted by intracellular cytoskeletal structures, since the surrounding plasma membrane is very pliable. Having a cell wall and a turgor pressure, living plant cells on the other hand possess an exoskeleton and a hydrostatic skeleton in addition to the cytoskeleton. Both are likely to produce considerable resistance to mechanical deformation. Since deformations applied during

J.-F. Bolduc · L.J. Lewis
Département de Physique,
Université de Montréal,
C.P. 6128 Succursale Centre-Ville,
Montréal, QC, Canada, H3C 3J7

A. Geitmann (✉)
Institut de Recherche en Biologie Végétale,
Université de Montréal,
4101 rue Sherbrooke est,
Montréal, QC, Canada, H1X 2B2
E-mail: anja.geitmann@umontreal.ca
Tel.: +1-514-8728492
Fax: +1-514-8729406

C.-É. Aubin
Mechanical Engineering Department,
École Polytechnique de Montréal,
PO BOX 6079, Station Centre-ville,
Montréal, QC, Canada, H3C 3A7

micro-indentation are large enough to affect cell shape, the geometrical structure of the investigated cell as well as that of the indenting stylus need to be taken into consideration in the case of plant cells. The present work aims at developing a mechanical model for the interaction between plant cell and the micro-indentation stylus in order to be able to correctly analyze quantitative data obtained by micro-indentation of this type of cell. We used finite-element modeling to be able to accommodate complex cellular geometries in the future.

2 Micro-indentation

The micro-indenter performs local deformations on a cell and measures its resistive force as a function of the depth of the deformation. Similar to AFM, the technique is based on the cantilever principle; details of this instrument have been published elsewhere (Petersen et al. 1982; Zahalak et al. 1990). Briefly, a horizontal Vycor glass beam with known bending constant is controlled by a linear piezoelectric motor, which is programmed to perform vertical movements. A vertical cylindrical glass stylus attached to the free end of the Vycor glass beam makes contact with the cell. Optical sensors monitor the vertical positions of the stylus and the motor. The extent to which the Vycor glass beam is bent is proportional to the force exerted on the stylus by the cell and is determined by comparing tip displacements in the presence and absence of cell contact. This force is determined with the help of the force constant of the beam, which is obtained by prior calibration. The cellular stiffness is calculated from the slope of the linear part of the force–deformation graph.

3 The pollen tube as a model system

As a first attempt to model the interaction between the micro-indenter and a plant cell, we chose pollen tubes as a model system. These cells grow individually, thus are independent of surrounding tissues. They are readily manipulated for micro-indentation and their simple cylindrical geometry makes them an ideal object for modeling. Pollen tubes are the carriers of the male gametes in flowering plants. They are formed from a pollen grain upon contact with the stigma of a receptive flower. Their function is the transport of the gametes from the pollen grain to the ovule thus permitting fertilization.

Pollen tubes have a cylindrical shape with a diameter of 5–15 μm, depending on the plant species. Their length can reach several centimeters. The apex of the rapidly elongating cell is roughly hemisphere-shaped and all growth activity is confined to this region implying that the bulk of new cell wall material in the form of pectin polymers is added here. The result of this polar mode of growth is a cell wall, the thickness of which does not vary much around the cell (100–200 nm), but which shows a high degree of non-uniformity along the longitudinal axis concerning the distribution of its components. Methyl-esterified pectins are the major component in the apex, and pectins with a decreasing degree of esterification as well as cellulose and callose form the distal cell wall. This biochemical non-uniformity has long been purported to cause the apical cell wall to be less stiff than the distal regions – a mechanical prerequisite for the confinement of expansion to the apex.

While the structural and theoretical evidence for a softer cell wall at the apex is compelling, it is nevertheless circumstantial. It was only recently confirmed by mechanical experiments that the non-uniform distribution of physical properties of the cell wall might actually exist (Parre and Geitmann 2005a,b). Micro-indentation showed that local cellular stiffness is considerably lower at the apex of a growing pollen tube than at the distal part of the cell. In addition, viscoelastic behavior differed between the two parts of the cell. However, several structural features can be involved in the dramatic difference in cellular stiffness measured between the apical region and the shank of the pollen tube: (a) the almost complete absence of a substantial actin cytoskeleton in the apex, whereas a dense mesh of actin filament is present in the subapical area (Geitmann and Parre 2004); (b) the non-uniform distribution of cell wall components (Geitmann and Parre 2004; Parre and Geitmann 2005a); (c) the geometry of the cell which differs between the hemisphere-shaped apex and the cylindrical distal region. The last point is critical for the interpretation of the data obtained by micro-indentation, since it has the potential to mask effects caused by the non-uniform distribution of structural cellular molecules. Therefore, in this paper, we attempt to determine numerically how much the geometry of the cell influences quantitative measurements in micro-indentation experiments.

4 Objectives of the modeling approach

The following geometrical parameters will be considered when analyzing the effect of geometry on quantitative data obtained by micro-indentation experiments on pollen tubes: a) cellular geometry (hemisphere vs. cylinder), (b) radius of the cylindrical cell, (c) thickness of the cell wall, (d) radius of the indenting stylus. The first is pertinent for the evaluation of semi-quantitative data already published (Geitmann and Parre 2004; Parre and Geitmann 2005a,b), whereas the others will be pivotal for future quantitative approaches to determine the physical properties of pollen tubes and other cylindrical cells such as root hairs, fungal hyphae and moss protonemata. Therefore, the objective of this paper is to use modeling to obtain quantitative micro-indentation data showing the effect of each of the four parameters mentioned above.

5 Finite-element model of the interaction between pollen tube and micro-indenter

We chose finite-element methods to model the interaction between pollen tube and micro-indenter because they allow us to control and isolate geometrical parameters in a much better way than what can be done experimentally. We used the program ANSYS 8.0 (ANSYS Inc.) for its non-linear

analysis capabilities like the large deformation and contact algorithms which are required to solve our problem. In a micro-indentation experiment, the cell lies on a flat rigid surface (the glass bottom of the experimental chamber). A rigid object (the stylus of the micro-indenter) can be placed at various positions on the top of the cell and moved downward, thus compressing the cell against the underlying substratum. The finite-element model is composed of these three parts. The central part is the pollen tube; its representation as a finite-element model will change according to the question to be answered, as detailed below. The bilateral symmetry allows us to reduce the number of nodes and elements by modeling only half of the structure. The figures show the complete model, however.

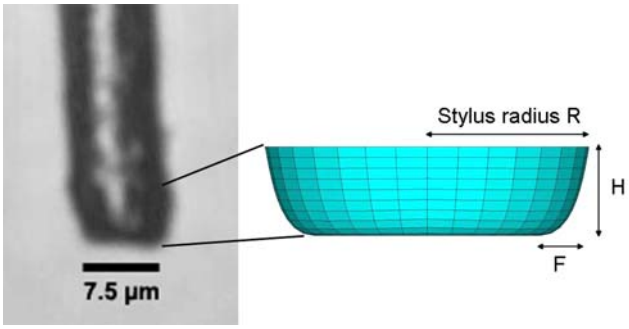

Fig. 1 Micro-indenter stylus seen in the optical microscope (*left*) and finite-element model used for the simulations (*right*). When varying the stylus radius (R) in the models, we kept the ratio F/R at 30% and H/R at 55%

5.1 Contact areas

The finite-element problem at hand necessitates the generation of two contact pairs. A contact pair consists of two surfaces, one called the target surface and the other called the contact surface, made of special elements designed to detect, control and perform contact between parts of a finite-element model. Here, both could be considered as rigid-to-flexible since the cell is a soft deformable object. TARGE170 elements (three nodes, triangular plane shape) are used for the rigid surfaces (indenter and substrate) that form one part of a contact interface. The other part is made of CONTA173 elements (three nodes, triangular plane shape) covering possible regions of contact on the pollen tube with each rigid surface (for the stylus, the upper half of the tube twice as large as the indenter, and for the substrate, the lower half of the tube).

5.2 Micro-indenter stylus

The micro-indenter stylus consists of a glass cylinder and is the part of the micro-indenter apparatus that makes contact with the cell. Its shape was approximated by a rigid surface made of 256 TARGE170 elements, 283 nodes and 1 pilot node. A pilot node is a special element consisting of a single node and used to control the movement of its associated rigid target surface, like a handle. It allows the displacement to be applied and the resistive force to be obtained at this particular node for the entire rigid surface that is associated with it. The stylus radius was set to $R = 5.5$ µm in all analyses that did not involve a change in this parameter. Other stylus dimensions (see Fig. 1) were set according to the following ratios, F/R at 30% and H/R at 55% which where chosen to approximate the real shape of the indenter. These ratios were kept constant when varying the stylus radius. To simulate the indentation process a vertical (downward) displacement of 2.0 µm (with initially no space between the indenter and the tube) was imposed on the pilot node while keeping all other degrees of freedom fixed at zero (see Sect. 5.6 for the analysis procedure).

5.3 Glass bottom

The glass bottom of the experimental chamber on which the pollen tube lies is represented by the rigid substratum. In the model, it only has to be large enough to support the compression of the tube by the stylus. The width of the rigid substratum was chosen to be as large as the tube diameter and its length to be longer than the tube by one time its radius. The substratum ends flush with the distal end of the tube and protrudes at the apex. A total of 204 nodes and 150 TARGE170 elements plus 1 pilot node were used (Fig. 2). Using the pilot node, all degrees of freedom of the substratum were fixed to zero thus preventing any movement of the substrate.

5.4 Pollen tube

The present approach focuses on finding the role of geometrical parameters of the pollen tube cell and micro-indenter apparatus for micro-indentation results. More specifically,

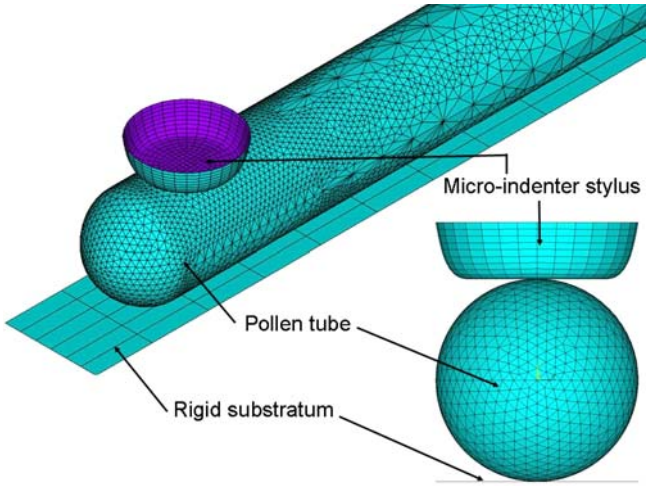

Fig. 2 Isometric view (*upper left*) and front view (*lower right*) of a typical finite-element representation of the three parts composing the model of the micro-indentation experiment on a pollen tube

our goal is to quantify the influence of pollen tube geometry, radius, cell wall thickness and micro-indenter stylus radius. Considering the type of questions asked, a simple model of the pollen tube seems appropriate. The regions of interest for our micro-indentation simulations are far from the pollen grain, at a distance of at least 200 μm. The grain is therefore very unlikely to influence our results and therefore was not modeled (see Sect. 5.5).

Any cytoplasmic structures, such as cytoskeletal elements and turgor, were neglected. We considered the cell wall in the model, because its features are the object of biological studies in our laboratory. Plant cell mechanical models previously proposed by other researchers share common global features, the plant cell wall being a major structural component. Although the mechanical properties of the cell wall for elongating cells are believed to be anisotropic, no mathematical formulation exists to describe it (Bruce 2003). Therefore our model consists of an isotropic homogeneous linear elastic membrane, as suggested by Bruce (2003) and used by many others (Hettiaratchi and O'Callaghan 1974; Pitt and Davis 1984), future studies might include cell wall inhomogeneity. It surrounds a linear elastic core, also isotropic and homogeneous. Throughout the four analyses, physical parameters were kept constant; they are shown in Table 1. The Young's modulus and Poisson's ratio of the cell wall were obtained from published data on the mechanical properties of primary plant cell wall analogues like cellulose/pectin composites (Chanliaud et al. 2002). Wang et al. (2004) reported that the Poisson's ratio of the shell had very little effect on force-deformation data from modeling compression of spherical plant cells; they used 0.4. We used the value of 0.3 given in Chanliaud et al. (2002). Estimations of the Young's modulus for plant cell walls span one order of magnitude, from several hundreds MegaPascal to a few GigaPascal (Wang et al. 2004); our 185 MPa value is taken from the same paper as the Poisson's ratio, and corresponds to the lower end of that range. While the living pollen tube is filled with cytoplasm – an aqueous solution, we modeled it as a solid. To mimic the behavior of water we set its physical properties to produce a small resistance to shear and elongation but large resistance to compression (high bulk modulus).

The pollen tube geometry is idealized by a 150 μm-long cylindrical shell capped at one end by a hemispherical shell of the same radius representing the apex (Fig. 2); the other end is flat. Table 2 shows the standard values of the geometrical parameters used in the model and the range of tested values to evaluate their role. The tube length was identical in all analyses.

Table 1 Values of the physical parameters which are kept constant for all models throughout the four analyses

Cell wall		Core	
Young's modulus	Poisson's ratio	Young's modulus	Poisson's ratio
185 MPa	0.3	1 Pa	0.49

Table 2 Parameters used in the present model

	Pollen tube (μm) radius	Cell wall (nm) thickness	Stylus (μm) radius
Standard value	3	200	5.5
Range of tested values	3–7	100–300	1.5–5.5

The range of tested values is limited to those that are biologically and technically relevant

While the range of values for the different structural features represents the variability encountered in different plant species, the dimensions used for standard cell wall thickness (200 nm) and pollen tube radius (3 μm) (Table 2) are those of a typical *Solanum chacoense* pollen tube – the species used in previous publications employing micro-indentation.

Generation of the mesh was done with ANSYS free meshing algorithm. The tube's core was meshed first using ANSYS SOLID185 elements (eight nodes, 3D structural solid) in tetrahedral shape. The region of the tube beneath the stylus had a denser mesh with element size approximately 1/10 of the stylus radius; element size in the regions away from the deformation zone could reach the tube's radius. The cell wall membrane was made of SHELL181 elements (four nodes, structural shell) generated around the core thus using the same nodes already at the surface of the tube which are attached to the solid elements. However, the rotational degrees of freedom of the shells could not be transferred to the solid elements because they do not have these degrees of freedom. The number of nodes (between 4,000 and 10,000) and elements (between 20,000 and 50,000) present in the pollen tube model were highly dependent on its dimensions, the position and the radius of the stylus.

5.5 Boundary conditions

A plane of bilateral symmetry was used along the longitudinal axis of the model. Fixed boundary conditions were set at the flat end of the tube. In the micro-indentation experiments the tubes are glued to the bottom of the experimental chamber using poly-L-lysine or stigmatic exudate. Therefore, for the nodes located at the bottom line of the tube, which are in contact with the rigid substrate prior to indentation, all three translational degrees of freedom were set to zero. This boundary condition prevents the tube from rigid body motion.

5.6 Vertical stylus displacement and type of analysis

Simulation of the micro-indentation process was done by imposing a vertical downward displacement on the surface representing the micro-indenter stylus and measuring the resistive force exerted on it by the tube. The contact problem and expected large deformation of the tube make the problem highly non-linear. Therefore, the total displacement of 2.0 μm was applied by increments of 0.2 μm, each of these

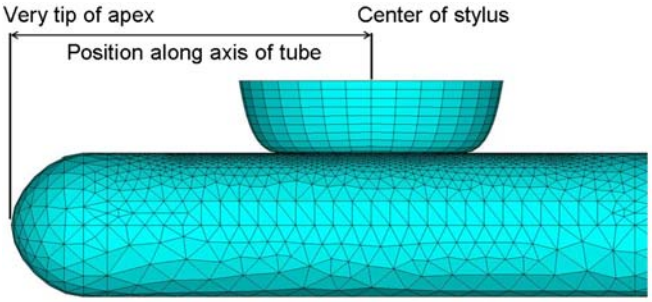

Fig. 3 Determination of positions along the tube's longitudinal axis

representing a load step. Since all materials in the model are time-independent, a quasi-static analysis could be used and we solved it using the sparse solver and the Newton–Raphson iterative method provided in ANSYS.

5.7 Positions along the pollen tube

The position of the micro-indenter stylus along the longitudinal axis of the tube was determined as follows. The position of the stylus was defined as the distance between the very tip (position zero) of the pollen tube apex and the center of the stylus (Fig. 3). For the three parameters, pollen tube radius, cell wall thickness and stylus radius, indentations were performed at two positions, one at 5 μm thus indenting the tube were its geometry undergoes a change in shape passing from a cylinder to a hemisphere, and another at 35 μm deforming the tube where its shape is a cylinder. In the following these two positions will be called apex and distal, respectively. This choice of positions was motivated by the shape difference mentioned above as well as by the results presented below showing the variation of stiffness along the tube's longitudinal axis. For the investigation of the role of the pollen tube radius, these positions have to be adjusted to compensate for the longer (or shorter) hemisphere that a change in tube radius implies. The apex 5 μm and distal 35 μm positions were chosen for a tube radius of 3 μm. Increasing the tube radius required an increase of both positions by the same amount in order to compare only the effect of pollen tube radius and not that of the change in position of the stylus due to the change in length of the tube. For example, for a tube radius of 4 μm the positions were 6 and 36 μm for the apex and distal positions, respectively.

6 Definition of stiffness

Previous publications of micro-indentation data on pollen tubes (Geitmann and Parre 2004; Geitmann et al. 2004; Parre and Geitmann 2005a,b) defined the stiffness of the tubes as the slope of the linear part of the force-displacement graphs at constant maximal deformation depth. A similar definition was given by Petersen et al. (1982) for micro-indentation on fibroblasts and by Mitchison and Swann (1954) for compression tests on sea urchin eggs. This method could not be used for our finite-element results because we do not have enough data points to clearly identify the linear part of the curve. Since in the experiments the linear part generally corresponded to the interval between 1.0 and 2.0 μm of vertical displacement of the stylus, we chose to do a linear regression on this portion of our theoretical force–displacement graphs. The obtained slope was defined as the stiffness of the tube.

7 Results

7.1 Geometry of the tube

Using the finite-element model we calculated the stiffness of the pollen tube at discrete positions, from 5 to 50 μm (see Sect. 5.7), along its longitudinal axis. Figure 4 shows that the stiffness is high at the apex and decreases rapidly between 5 and 16 μm from the apex whereas further away it remains approximately constant. The stiffness at the apex (5 μm) is almost fivefold higher than the distal (35 μm) value. This result reveals the impact of the difference in geometry between the apex and the distal region on the pollen tube's resistance to lateral deformation by micro-indentation.

7.2 Pollen tube radius

The pollen tube radius varies from one species to another; investigating the influence of this parameter will reveal how experimental results should be interpreted when comparing species with different radii. Figure 5a and b shows the force-displacement curves for various pollen tube radii for the apex (a) and the distal (b) regions. In Fig. 5c and d we can observe that smaller pollen tubes offer more resistance to deformation in both regions. The stiffness is three and five times higher for the apical and distal positions, respectively, when going from a 7 to a 3-μm-pollen tube radius.

7.3 Cell wall thickness

Previous studies on compression of spherical plant cells have demonstrated that the thickness of the cell wall plays an important role in the resistance to deformation (Wang et al. 2004). Electron microscopical analysis of this parameter for pollen tubes has revealed that it is generally within a range of 100 to 200 nm. This range of values contains sufficient uncertainty to warrant analysis of the effect of cell wall thickness on stiffness. We tested five different thicknesses: 100, 150, 200, 250 and 300 nm. The cell wall was composed of shell elements (SHELL181 in ANSYS) of constant thickness, i.e., for each of the simulations there was no thickness variation along the tube (nor was there any variation in mechanical

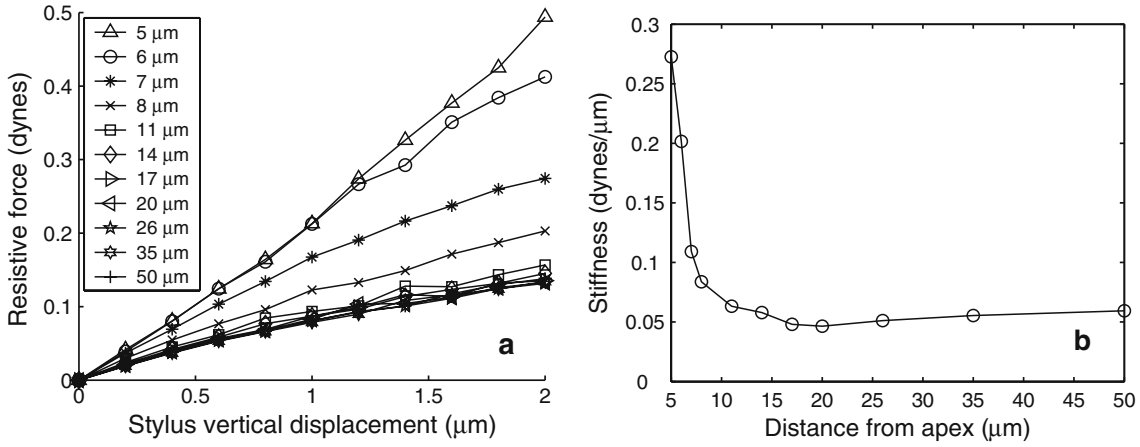

Fig. 4 **a** Force–displacement curves of micro-indentation simulations at different positions along the longitudinal axis of the tube. The legend gives these positions in micrometers calculated from the very tip of the apex. **b** Stiffness of the cell (*y*-axis) plotted against position on the tube (*x*-axis, corresponding to the positions given in the legend of **a**)

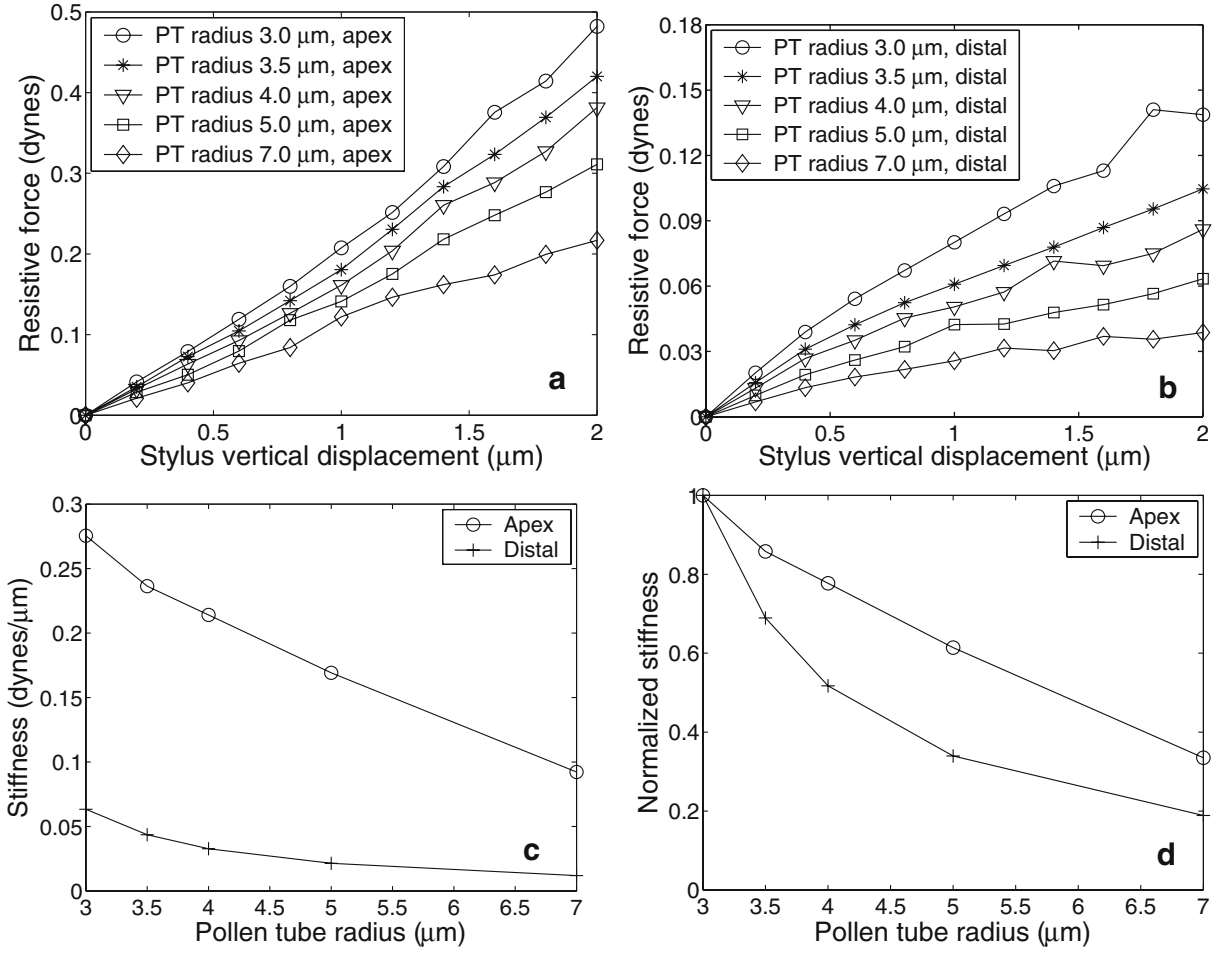

Fig. 5 **a, b** Influence of pollen tube (PT) radius on force–displacement curves for the apex and distal regions, respectively. **c, d** Stiffnesses for pollen tube radius varying from 3 to 7 μm

properties). The effect of thickness was investigated at two positions on the tube, the apex and distal, as shown in Fig. 6. As expected, changing the thickness of the cell wall affects the stiffness of the cell, the apex stiffens by a factor of 4 and the distal region by a factor of 27 when increasing the thickness from 100 to 300 nm.

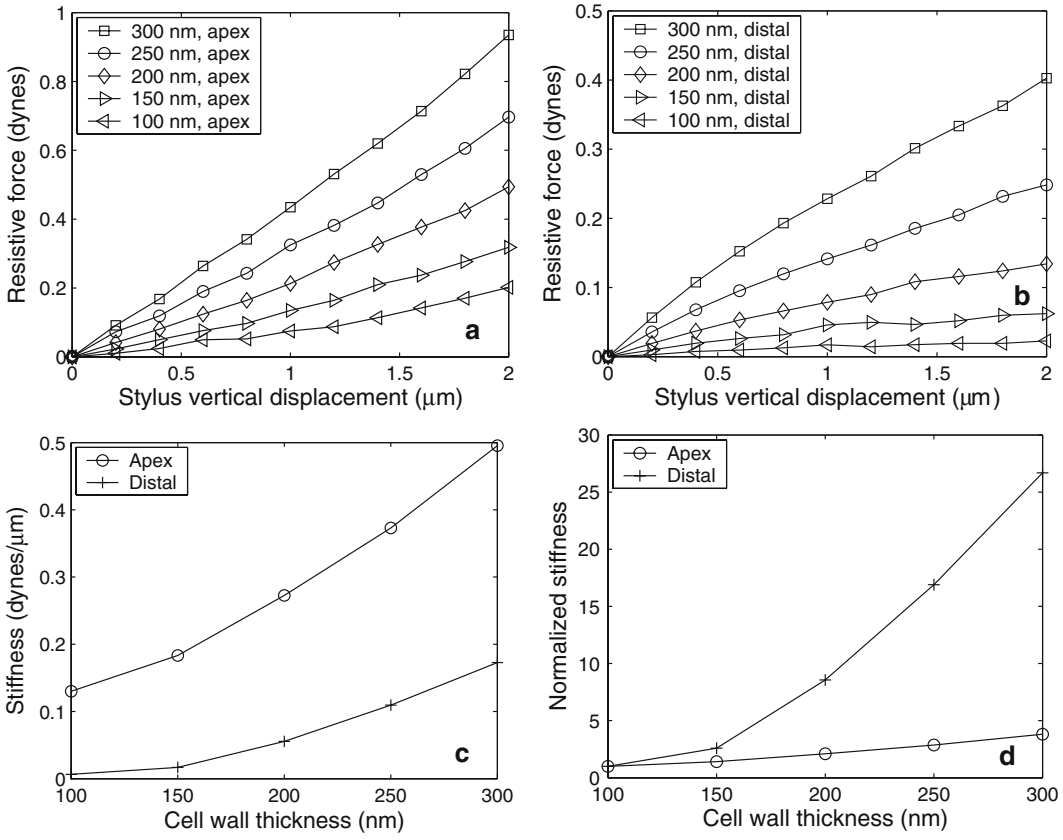

Fig. 6 a, b Influence of the cell wall thickness on force–displacement curves for the apex and distal regions, respectively. **c, d** Stiffnesses for cell wall thickness varying from 100 to 300 nm

7.4 Radius of the micro-indenter stylus

The real micro-indenter stylus is made of glass; its dimensions and shape make it a very fragile component of the micro-indenter apparatus. It can easily be broken and thus needs to be replaced. Producing a stylus of exactly the same size and shape is rather difficult with the procedure presently used. Therefore, we wanted to know to what degree stiffness values are influenced by the diameter of the stylus. For both the apex and distal regions, the apparent stiffness increases significantly when the stylus radius is increased from 1.5 to 5.5 μm (Fig. 7). However, with a fivefold increase the effect is greater at the apex than at the distal region which only showed a twofold increase. Interestingly, the apex showed a much steeper increase in stiffness for a stylus radius higher than 3.5 μm which is nearly equal to the standard 3 μm pollen tube radius used for the analysis. The stiffness in the distal part on the other hand showed a smooth linear increase.

8 Discussion

We analyzed four geometrical parameters that might have an influence on the values measured for the stiffness of cylindrical plant cells such as pollen tubes using micro-indentation. The first parameter is the tube geometry, which changes from hemispherical to cylindrical when moving from the apex to the distal region. Previously, we had shown that the stiffness of the pollen tube exhibits a gradient along the longitudinal axis (Geitmann and Parre 2004). Starting with a lower value at the apex the stiffness increases rapidly within the first 20 μm of the tube and then remains approximately constant further away from the apex. In *S. chacoense* pollen tubes, which is the species on which the geometrical parameters in this modeling approach are based on, the distal stiffness amounted to around 0.48 dynes/μm, whereas the apical stiffness was around 0.41 dynes/μm, thus significantly lower (Parre and Geitmann 2005a). In other species this difference is even more pronounced (Geitmann and Parre 2004). We wanted to know whether this effect was partly or maybe even completely due to the geometry of the cell as opposed to the gradient in the biochemical composition of the cell wall. Our model shows a behavior that is opposite to that of the experimental data. In a hypothetical tube with uniform cell wall properties, the apex is expected to be much stiffer than the tubular distal part. If anything, geometry therefore masks part of the softening effect that the biochemical gradient has on living pollen tubes. With a stiffness of 0.05 dynes/μm in the distal part and 0.27 dynes/μm in the apex, the values obtained by our modeling approach are in the same order of magnitude but not identical to the experimental values. This

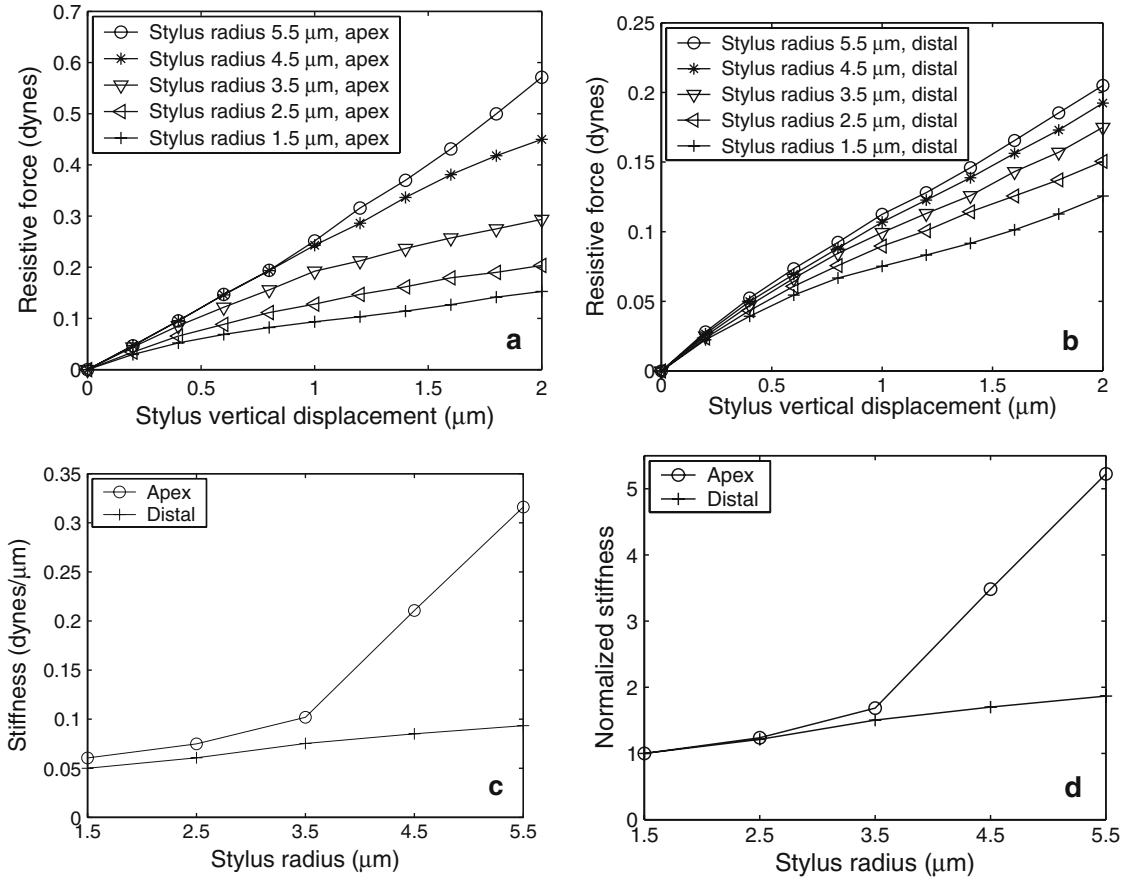

Fig. 7 a, b Influence of the radius of the micro-indenter stylus on force-displacement curves. **c, d** Stiffnesses for stylus radius varying from 1.5 to 5.5 μm

is probably due to several factors: the turgor pressure is not considered in the model, and the physical parameters for the mechanical cell wall properties are not based on experimental data specifically from pollen tubes but more general material properties obtained from literature. Nevertheless, the fact that the values obtained with our model are in the correct order of magnitude allows us to conclude that this is a good model to start out with when building a more complex version.

The pollen tube radius is rather stable in *in vitro* cultures of individual species but varies considerably between species. Therefore we wanted to investigate how changes in pollen tube radius could affect micro-indentation results. We compared a range of pollen tube radii that can be encountered in the plant species generally used in our lab. Our simulations reveal a strong influence of the radius on the values measured for stiffness with augmentation as high as threefold for the apex and fivefold for the distal region when comparing a pollen tube with a 3 μm radius to another one having a 7 μm radius. These values represent the extremes on a biologically relevant range of pollen tube dimensions. Keeping all other variables constant, smaller tubes are therefore stiffer. This is not surprising, since if the absolute wall thickness is kept constant, the ratio between wall thickness and tube radius is bigger in smaller tubes. However, even if we look at the presumed small variability of the radius within a single species (estimated to be around ±10% of the average value), our results show that we must expect a considerable effect on stiffness. For example, the stiffness decreases by 9 and 19% for the apex and distal regions, respectively (Table 3), for a pollen tube radius 10% bigger than 3 μm that would be the typical value for *S. chacoense* pollen tubes. Interestingly, the relationship between stiffness and pollen tube radius appears almost linear for the apex region, whereas it was rather nonlinear for the distal one (Fig. 5d). The decrease of 19% for the distal part corresponds to the steepest part of the curve. This implies that species with larger radii should show a smaller variability within a population of cells.

Cell wall thickness in vivo is rather constant. However, according to our model an estimated variability of ±10% in thickness in the cell wall of a single pollen tube could result in changes in stiffness of approximately ±15 and ±35% for apex and distal regions, respectively (Table 3). The stiffness curves are almost linear except for cell wall thicknesses lower than 150 nm, as shown in Fig. 6d. Even more dramatic were the changes observed for the range of thicknesses investigated (100–300 nm) which showed an increase by a factor of

Table 3 Summary of results

Stiffness	Tube geometry	Pollen tube radius	Cell wall thickness	Stylus radius
Apex (5 μm)	492% of distal value	7 → 3 μm (↗ 298%)	100 → 300 nm (↗ 381%)	1.5 → 5.5 μm (↗ 522%)
−10% Standard value	Does not apply	Value not available	↘ 15%	Does not apply
+10% Standard value	Does not apply	↘ 9%	↗ 14%	Does not apply
Distal (35 μm)	20% of apex value	7 → 3 μm (↗ 530%)	100 → 300 nm (↗ 2669%)	1.5 → 5.5 μm (↗ 187%)
−10% Standard value	Does not apply	Value not available	↘ 33%	Does not apply
+10% Standard value	Does not apply	↘ 19%	↗ 36%	Does not apply

↗ (↘) X% means increase (or decrease) of the stiffness by X%

4 in apex stiffness and by a factor of 27 for the distal region. These results demonstrate clearly that the cell wall thickness is a very important variable that strongly influences micro-indentation results. As a consequence, drug or enzyme treatments used to alter cell wall biochemistry need to be carefully analyzed for their effect on cell wall thickness.

In the past, while we worked with different sizes of stylus, we never changed the stylus within a series of experiments. This care proves to be sensible, since the model shows that the stiffness measurements made at the apex were highly sensitive to the size of the stylus when its radius exceeds that of the cell. The standard value of pollen tube radius being 3 μm, two linear parts could be distinguished in the stiffness curve for the apex. The first exhibiting a raise by a factor of 1.7 between 1.5 and 3.5 μm and the second a much steeper increase by a factor of 3 between 3.5 and 5.5 μm for an overall fivefold increase in stiffness for the total range of stylus radii tested (Fig. 7d). On the other hand, measurements at the distal region were less affected by the stylus radius but still did show a noticeable linear twofold increase in stiffness between 1.5 and 5.5 μm stylus radius. Obataya et al. (2005) demonstrated that the shape of the indenter used in AFM has an important impact on the probability of penetration of a cellular membrane. Albeit not being directly applicable to our experimental system, this finding is consistent with our results.

Simulation results also indicate that experimental values of stiffness can only be evaluated in a semi-quantitative manner to indicate changes as opposed to absolute values. In the past we have interpreted our data correspondingly. Modeling shows that none of the four factors could be neglected in the interpretation of experimental results. A summary of these results is presented in Table 3, quantification of stiffness variations are given for the four parameters at the two positions previously mentioned and variation of ±10% around standard value are also indicated were applicable/available.

Another parameter that is likely to influence experimental deformation values is the exact position of the stylus. Both in the experiments and in our model we presume that deformation always occurs on the center line of the tube. Due to our experimental setup this position can be controlled rather precisely by microscopical observation, but it would certainly be interesting to investigate the sensitivity of the experimental data to the variations in the position of the stylus in the direction perpendicular to the longitudinal axis of the pollen tube.

Another limitation of our present model is the fact that the mechanical properties of the pollen tube cell wall and core are only approximations. Furthermore, the model is extremely simplified, since it neglects an important feature of plant cells, the turgor pressure. Considering the cell wall as a linear, homogeneous and isotropic elastic shell the model neglects any anisotropic properties the cell wall might have. It is therefore comparable to the model developed by (Cheng 1987a,b), which modeled, using finite-element method, the compression of a spherical shell containing an incompressible material. Interestingly, the authors prestretched the membrane, whereas our present model does not. Further approaches should include the presence of the turgor pressure by modeling the pollen tube as a shell inflated under an internal pressure. That type of mathematical model has already been proposed for the spherical non-linear membrane applicable to sea urchin eggs (Feng and Yang 1973; Lardner and Pujara 1980), microcapsules (Liu et al. 1996), yeast cells (Smith et al. 1998) and tomato cells (Wang et al. 2004). Zhao et al. (2005) demonstrated experimentally and by using FE modeling that turgor pressure does not affect indentation of hyphae by AFM. However, deformations using AFM have a much smaller amplitude (in the order of nanometers) than those done by micro-indentation (in the order micrometers) and are furthermore performed by an indenter of extremely small dimension that is considered as a point force compared to the size of the deformed cell. We therefore think that contrary to AFM deformations, our micro-indentations will need to consider turgor as a factor influencing deformation curves and will incorporate this parameter in a future version of the model. While the present model is certainly limited, it has however provided us with information that is essential for the development of our experimental approaches. It has shown that within their biologically or technically relevant ranges all parameters investigated here – cell geometry, pollen tube radius, cell wall thickness and micro-indenter stylus radius – need to be considered as influential elements in the interpretation of micro-indentation results.

Acknowledgements This work was supported by grants from the Natural Sciences and Engineering Research Council of Canada (NSERC) and the *Fonds Québécois de la Recherche sur la Nature et les Technologies* (FQRNT).

References

A-Hassan E, Heinz WF, Antonik MD, D'Costa NP, Nageswaran S, Schoenenberger C-A, Hoh JH (1998) Relative microelastic mapping of living cells by atomic force microscopy. Biophys J 74:1564–1578

Bao G, Suresh S (2003) Cell and molecular mechanics of biological materials. Nat Mater 2:715–725, DOI 10.1038/nature0110.1038/nmat1001

Bruce DM (2003) Mathematical modelling of the cellular mechanics of plants. Philos Trans R Soc Lond Biol Sci 358:1437–1444, DOI 10.1098/rstb.2003.1337

Chanliaud E, Burrows KM, Jeronimidis G, Gidley MJ (2002) Mechanical properties of primary plant cell wall analogues. Planta 215:989–996, DOI 10.1007/s00425-002-0783-8

Cheng LY (1987a) Deformation analysis in cell and developmental biology. Part I-Formal methodology. J Biomech Eng 109:10–17

Cheng LY (1987b) Deformation analysis in cell and developmental biology. Part II-Mechanical experiments on cells. J Biomech Eng 109:18–24

Feng WW, Yang W-H (1973) On the contact problem of an inflated spherical nonlinear membrane. J Appl Mech 41:209–214

Fabry B, Maksym GN, Butler JP, Glogauer M, Navajas D, Fredberg JJ (2001) Scaling the microrheology of living cells. Phys Rev Lett 87(14):148102, DOI 10.1103/PhysRevLett.87.148102

Geitmann A, Parre E (2004) The local cytomechanical properties of growing pollen tubes correspond to the axial distribution of structural cellular elements. Sex Plant Reprod 17:9–16, DOI 10.1007/s00497-004-0210-3

Geitmann A, McConnaughey WB, Lang-Pauluzzi I, Franklin-Tong VE, Emons AMC (2004) Cytomechanical properties of *Papaver* pollen tubes are altered after self-incompatibility challenge. Biophys J 86:3314–3323

Hettiaratchi DRP, O'Callaghan (1974) A membrane model of plant cell extension. J Theor Biol 45:459–465

Jones WR, Ting-Beall HP, Lee GM, Kelley SL, Hochmuth RM, Guilak F (1999) Alterations in the Young's modulus and volumetric properties of chondrocytes isolated from normal and osteoarthritic human cartilage. J Biomech 32:119–127

Lardner TJ, Pujara P (1980) Compression of spherical cells. Mech Today 161–176

Lintilhac PM, Wei C, Tanguay JJ, Outwater JO (2000) Ball tonometry: a rapid, nondestructive method for measuring cell turgor pressure in thin-walled plant cells. J Plant Growth Regul 19:90–97, DOI 10.1007/s003440000009

Liu KK, Williams DR, Briscoe BJ (1996) Compressive deformation of a single microcapsule. Phys Rev E 54(6):6673–6680

Mitchison JM, Swann MM (1954) The mechanical properties of the cell surface I. The cell elastimeter. J Exp Biol 31(3):443–460

Obataya I, Nakamura C, Han SW, Nakamura N, Miyake J (2005) Mechanical sensing of the penetration of various nanoneedles into a living cell using atomic force microscopy. Biosens Bioelectron 20:1652–1655

Parre E, Geitmann A (2005a) Pectin and the role of the physical properties of the cell wall in pollen tube growth of *Solanum chacoense*. Planta 220(4):582–592, DOI 10.1007/s00425-004-1368-5

Parre E, Geitmann A (2005b) More than a leak sealant: the mechanical properties of callose in growing plant cells. Plant Physiol 137:274–286, DOI 10.1104/pp.104.050773

Pitt RE, Davis DC (1984) Finite element analysis of fluid-filled cell response to external loading Trans Am Soc Agric Eng 27:1976–1983

Petersen NO, McConnaughey WB, Elson EL (1982) Dependence of locally measured cellular deformability on position on the cell, temperature, and cytochalasin b. Proc Natl Acad Sci USA 79:5327–5331

Shin D, Athanasiou K (1999) Cytoindentation for obtaining cell biomechanical properties. J Orthop Res 17(6):880–890

Smith AE, Moxham KE, Middelberg APJ (1998) On uniquely determining cell-wall material properties with the compression experiment. Chem Eng Sci 53(23):3913–3922

Tomos D (2000) The plant cell pressure probe. Biotechnol Lett 42:437–442

Thomas CR, Zhang Z, Cowen C (2000) Micromanipulation measurements of biological materials. Biotechnol Lett 22:531–537

Wang CX, Wang L, Thomas CR (2004) Modelling the mechanical properties of single suspension-cultured tomato cells. Ann Bot 93:443–453, DOI 10.1093/aob/mch062

Wei C, Lintilhac PM, Tanguay JJ (2001) An insight into cell elasticity and load-bearing ability. Measurement and theory. Plant Physiol 126:1129–1138

Zahalak GI, McConnaughey WB, Elson EL (1990) Determination of cellular mechanical properties by cell poking, with an application to leukocytes. J Biomech Eng 112:283–294

Zhao L, Schaefer D, Xu H, Modi SJ, LaCourse WR, Marten MR (2005) Elastic properties of the cell wall of *Aspergillus nidulans* studied with atomic force microscopy. Biotechnol Prog 21:292–299